e-ISSN: 2682-8588

PENERBIT PRESS
UNIVERSITI TEKNOLOGI MARA

Available online at
https://journal.uitm.edu.my/ojs/index.php/MJCET

Malaysian Journal of Chemical Engineering & Technology 9(1) 2026, 52–64

Malaysian Journal of Chemical Engineering and Technology

Computational study of nozzle configuration of jet impingement heat transfer on concave surface

Nurul Hyidayah Shahrin[1], Nadia Kamarrudin[2*], Masli Irwan Rosli[3], Mohd Fadhil Majnis[4]

[1,2,4]*Faculty of Chemical Engineering, Universiti Teknologi MARA, 40450, Shah Alam, Selangor, Malaysia*
[2,3]*Faculty of Engineering and Built Environment, Universiti Kebangsaan Malaysia, 43600, Bandar Baru Bangi, Selangor, Malaysia*

ARTICLE INFO

Article history:
Received 7 November 2025
Revised 10 February 2026
Accepted 10 February 2026
Online first 29 April 2026
Published 30 April 2026

Keywords:
Jet Impingement
Heat transfer
Concave surface
CFD
Turbulence kinetic energy

DOI:
10.24191/mjcet.v9i1.9004

ABSTRACT

Jet impingement has been actively utilised in many applications for cooling and drying as it gives high heat transfer coefficient. This technique has proven highly effective in eliminating excessive thermal loads, such as the leading edges of turbine blades and the outer walls of combustors. This study investigates turbulent jet impingement cooling on a concave surface with a focus on how jet to surface spacing and Reynolds number govern hydrodynamics and heat transfer. A validated Reynolds averaged Navier–Stokes model with constant wall heat flux and a mesh independent solution was used to map area averaged Nusselt number and turbulent kinetic energy near impingement. The findings show strong dependence on the small jet-to-surface distance, H/B (0.50). An increasing nozzle diameter from 5 to 15 mm increases the Nusselt number from 86.58 to 170.77 (97% increase) and turbulent kinetic energy from 82.28 to 1093.91 $m^2 \cdot s^{-2}$. H/B is the dominant control parameter at fixed diameter. The Nusselt number decreases from 170.77 at H/B = 0.50 to 71.69 at H/B = 8.00 for 15 mm nozzle diameter which is a 58% reduction. Increasing Reynolds number strengthens turbulence at the impingement region, improves mixing, enlarges the effective cooling area, and aligns with higher Nusselt number. These findings indicate a preference for small to moderate jet-to-surface distance with sufficiently high Reynolds numbers for concave targets and support energy efficient thermal management in advanced industrial systems.

1. INTRODUCTION

Jet impingement cooling is widely used in industry due to its effectiveness in removing localised heat loads and improving thermal management performance. Jet impingement cooling techniques were developed to

[2*]Corresponding author. *E-mail address*: nadia3132@uitm.edu.my

help industries deal with the growing problem of managing heat flow efficiently in high-heat conditions. These problems made it necessary to find localised and high-performance cooling solutions that could meet strict thermal control needs. Computational studies have become a powerful tool for simulating complex flow and heat transfer phenomena in order to improve understanding and optimisation of jet impingement systems.

The geometrical configuration of an impinging jet has a significant impact on the thermal performance of the system. Ekkad & Singh (2021) comprehensively reviewed the jet impingement heat transfer enhancement techniques, highlighting the importance of geometric configuration and turbulence development in improving cooling performance. Parameters such as Reynolds number, nozzle configuration, and the distance between the nozzle and the impingement surface are important in determining the heat transfer distribution in an impinging jet system (Rakhsha et al., 2023; Prevost et al. 2022; Attalla & Salem, 2013). Nozzle diameter also plays a crucial role in determining heat transfer distribution in an impinging jet system, as they affect the jet properties and heat transfer rates. A number of experimental investigations and theoretical studies on heat transfer distribution in an impinging jet have been presented in the literature. For example, Baonga et al. (2006) studied the heat transfer distribution in an impinging jet system using a nozzle orifice diameter, which affects heat transfer distribution by varying the pressure drop in the nozzle, which in turn affects the velocity profile of the jet. Attalla & Salem (2013) studied the effect of nozzle edge chamfering on heat transfer distribution in an impinging jet system, where it was found that heat transfer distribution did not change significantly in the presence of a chamfered edge in the nozzle.

Moreover, Kund (2019) examined the influence of nozzle diameter on heat transfer performance in jet impingement cooling systems and reported that smaller nozzle diameters produce higher jet velocities, leading to more effective localised cooling. However, this enhancement in heat transfer was accompanied by a less uniform temperature distribution across the impingement surface. In a related study, Garimella and Nenaydykh (1996) analysed submerged and confined liquid jet impingement cooling systems and found that larger nozzle diameters produce higher turbulence intensity, which improves heat transfer rates in the stagnation region. In another investigation, Choo and Kim (2016) studied the effect of nozzle diameter on the hydraulic jump radius in jet impingement cooling systems. Their results showed that, at a constant Reynolds number, a reduction in nozzle diameter increases the dimensionless hydraulic jump radius. This behaviour was attributed to increased impingement power due to high pressure differences and flow rates in the jet impingement cooling system.

As the study of geometric parameters and their impact on impinging jets progressed, emphasis was given to improving jet performance through the Reynolds number. The Reynolds number is an important dimensionless parameter that determines the nature of fluid flow, whether it is turbulent or laminar, and its intensity. These parameters of fluid flow are directly related to the efficiency of heat transfer. Conahan (2021) has shown that the area-averaged value of the Nusselt number follows a power-law correlation with the Reynolds number. This proved that an increase in the Reynolds number will result in an increase in the heat transfer coefficient. Additionally, the effect of Reynolds number on jet impingement cooling performance over a semi-circular concave surface was experimentally investigated by Yang et al. (1999) using three alternative slot nozzle configurations. The study also indicates that concave surfaces have higher heat transfer rates than flat surfaces due to curvature-induced vortices. These vortices are formed due to centripetal forces acting on the jet.

Janajreh et al. (2014) furthered this knowledge with numerical analyses of various jet impingement arrangements on semi-circular surfaces. The results found that concave curvature leads to a significant enhancement in heat transfer efficiency, as indicated by the elevated average Nusselt numbers compared to flat surfaces. The influence of geometric variables on local heat transfer coefficients for circular jets impinging on concave surfaces was investigated further by Patil and Vedula (2018). More recently, Erasmus et al. (2021) used computational fluid dynamics simulations to analyse jet impingement on a concave hemispherical dome. Related computational studies by Basha et al. (2018) on slot jet impingement indicated that the Nusselt number reduces with an increase in the distance between the jet and the surface.

Overall, existing studies indicate that jet impingement cooling has strong potential to improve efficiency and cost effectiveness in thermal management applications involving concave surfaces. Nevertheless, despite the large number of experimental and numerical investigations reported in the literature, a systematic quantification of how jet impingement configurations influence heat transfer performance is still limited. In particular, the combined effects of geometric and flow parameters on concave surfaces remain insufficiently explored. Therefore, the objective of this study is to develop and validate a computational fluid dynamics model of jet impingement cooling on a concave surface. The study systematically quantifies the combined influence of geometric and flow parameters (nozzle configuration, jet to surface distance, and Reynolds number) on turbulent kinetic energy distribution and heat transfer characteristics. The findings of this research are expected to provide quantitative insights that support the optimisation of jet impingement cooling designs.

2. METHODOLOGY

2.1 Geometry modelling

The schematic design of the geometry is shown in Fig.1, where the dimensions of the computational domain are adapted from the experimental study by Yang et al. (1999). In the simulation study, a commercially available CFD package, ANSYS Fluent was used. The turbulent flow is assumed to be steady state, 2-D and incompressible with constant properties.

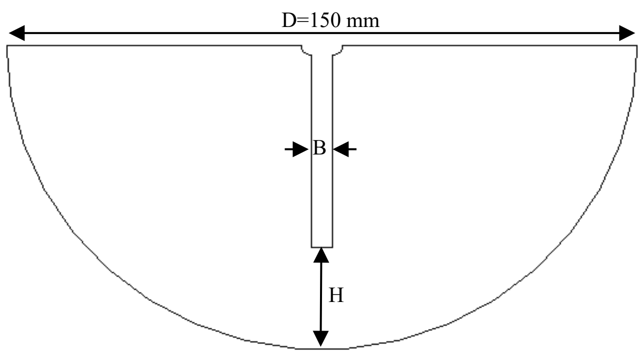

Fig.1. Computational domain

Source: Author’s illustration

2.2 Boundary conditions and mesh independency study

The design of jet impingement was set up on a semi-circular concave wall with a range of diameters from 5.0 to 15.0 mm, and the jet-to-surface distance, H/B, is 0.5 to 8. Air was used as a cooling medium. The model setup and parameters used are summarised in Table 1.

Table 1. The dimensions of jet impingement

Parameter	Conditions/values
Type of fluid	Air
Type of surface	Steel
Inlet velocity (m/s)	36.97
Jet-to-surface distance ratio (H/B)	0.5, 2, 5, 8
Surface diameter, D (mm)	150
Inlet diameter, B (mm)	5, 10, 15

Source: Author's own data

The domain is imported into the meshing environment to generate a computational grid that can resolve the governing flow and thermal gradients with sufficient reliability. Mesh design has a significant impact on solving flow physics with accurate, efficient, and reliable simulation results. Fig. 2 presents the generated grid for the semi-circular concave jet impingement configuration.

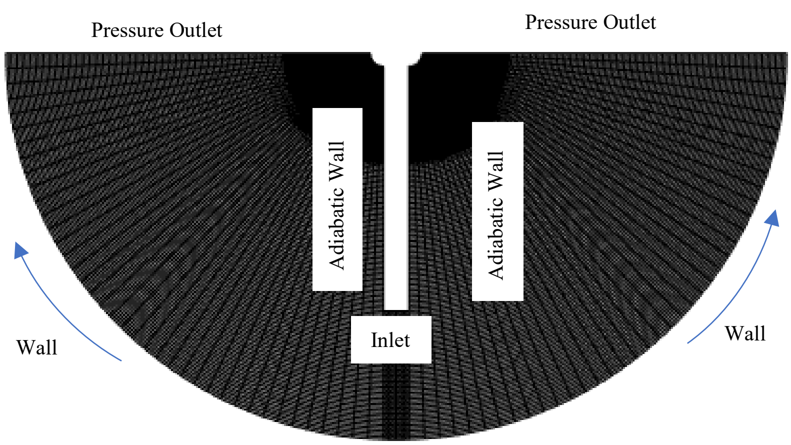

Fig. 2. Mesh structure and boundary condition

Source: Author's illustration

In order to test the model with a mesh independence test, different sizes of meshes were employed until the solution no longer varied with additional grid refinement and validated with literature data. As a result, a mesh independence test showed that the simulations based on a mesh of 21848 elements provide satisfactory numerical accuracy. The maximum changes in the predicted Nusselt number were 1.47%

between the mesh element numbers of 21848 and 22014 as shown in Fig. 3. Therefore, it can be considered as mesh independent.

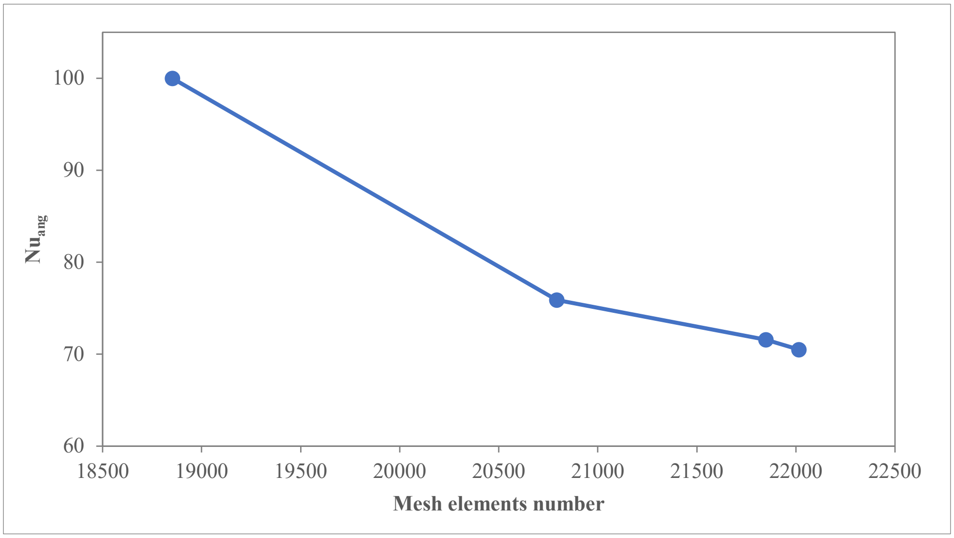

Fig. 3. Effect of mesh refinement on the average Nusselt number (H/B = 8, Re = 23700)

Source: Author's own data

2.3 Governing equations and solution scheme

In this study, a steady state solver was developed based on SIMPLE algorithm to model the heat transfer between the fluid and solid domains. To simulate the flow and thermal patterns within the geometry, the k-epsilon (k-ε) turbulence model was chosen throughout the domain as this study was conducted in turbulent flow. Thus, the conservative equations and turbulence model was outlined as follows (Versteeg & Malalasekera, 2007; Yang et al., 2011):

(1) Continuity equation

$$\frac{\partial u_i}{\partial x_i} = 0 \tag{1}$$

(2) Momentum equation

$$\rho u_j \frac{\partial \mathrm{u}_i}{\partial \mathrm{x}_\mathrm{i}} = -\frac{\partial p}{\partial \mathrm{x}_\mathrm{i}} + \frac{\partial}{\partial x_j}\left[\mu_i\left(\frac{\partial u_i}{\partial x_j} + \frac{\partial u_j}{\partial x_i}\right) - \rho u_i u_j\right] \tag{2}$$

where,

$$\rho u_i u_j = \mu_t\left(\frac{\partial u_i}{\partial x_j} + \frac{\partial u_j}{\partial x_i}\right) - \frac{2}{3}\delta_y \rho k \tag{3}$$

(3) Energy equation

$$\rho \mathrm{u}_j \frac{\partial T}{\partial x_j} = \frac{\partial}{\partial \mathrm{x_j}}\left[\left(\frac{\mu_l}{\sigma_l} + \frac{\mu_t}{\sigma_t}\right)\frac{\partial \mathrm{T}}{\partial \mathrm{x_j}}\right] \quad (4)$$

(4) Transport equation for k

$$\rho u_j \frac{\partial k}{\partial x_i} = \frac{\partial}{\partial x_j}\left[\left(\mu_l + \frac{\mu_t}{\sigma_k}\right)\frac{\partial}{x_j}\right] + \mu_l\left(\frac{\partial u_i}{\partial x_j} + \frac{\partial u_j}{\partial x_i}\right)\frac{\partial u_i}{\partial x_j} - \rho\varepsilon \quad (5)$$

(5) Transport equation for ε

$$\rho u_j \frac{\partial \varepsilon}{\partial x_j} = \frac{\partial}{\partial x_j}\left[\left(\mu_l + \frac{\mu_t}{\sigma_\varepsilon}\right)\frac{\partial \varepsilon}{x_j}\right] + C_1\mu_l\left(\frac{\partial u_i}{\partial x_j} + \frac{\partial u_j}{\partial x_i}\right)\frac{\partial u_i}{\partial x_j} - C_2\rho\frac{\varepsilon^2}{k} \quad (8)$$

where,

$$\mu_l = \rho C_\mu \frac{k^2}{\varepsilon} \quad (9)$$

The closure coefficients appear in the equations are given by the following values: $C_1 = 1.44$, $C_2 = 1.92$, $C_\mu = 0.09$, $\sigma_k = 1.44$, $\sigma_\varepsilon = 1.3$. A least-squares cell-based procedure was used for gradient discretisation to enhance derivative accuracy. A second order upwind formulation was adopted for the momentum, turbulent kinetic energy, and dissipation rate equations to control numerical dispersion and maintain stability. Convergence was attained when all equation residuals dropped below 1×10^{-6}.

2.4 CFD model validation

Model validation and boundary condition selection were supported by comparison of the present simulations with literature experiments for H/B = 8 and Re = 23700 by Yang et al. (1999).

2.5 Flow and thermal characteristics

The flow and thermal characteristics of jet impingement cooling were analysed as a function of nozzle diameter, Reynolds number, and jet-to-surface distance (H/B) to determine the cooling performance, as shown in Table 2.

Table 2. Design parameter

Parameter	Values
H/B	0.5, 2, 5, and 8
Nozzle diameter (mm)	5, 10, and 25
Reynold Number, Re	5000, 25000, and 45000

Source: Author’s own data

3. RESULTS AND DISCUSSION

3.1 CFD model validation

The validation was performed by comparing the average Nusselt number value obtained from the simulation with the experimental study by Yang et al. (1999). To ensure accuracy with the referenced study, the adapted geometry, working fluid (air), and constant heat flux conditions were applied. In line with the validation approach, the jet-to-surface distance (H/B) is varied at 0.5, 2, 5, and 8 using a nozzle diameter of 5 mm, to replicate the conditions of the original study. The results obtained from the simulation were presented and compared in Table 3.

Table 3. Relative error for CFD model validation

Jet-to-surface distance (H/B)	Average Nusselt number (Nu_{avg})		Relative percentage error (%)
	Yang et al. (1999)	Present study	
0.50	83.13	86.58	4.16%
2.00	70.94	76.18	7.39%
5.00	74.55	72.32	2.99%
8.00	72.19	71.56	0.87%
		Average	**3.85%**

Source: Author's own data

For validation, relative percentage errors were measured as indicated in Table 3. The differences between the CFD simulation and literature data ranged from 0.87 to 7.39%, with an average of 3.85%. The calculated average relative error reached a good agreement with a marginal difference of less than 10%. Therefore, it is worthy to mention that the simulation model developed in this study is very close to literature values. Hence, the developed model is suitable for the prediction of jet impingement heat transfer under specified cutting conditions.

3.2 Flow and thermal characteristics

Effect of jet-to-surface distance (H/B) ratio

The H/B ratio is an important parameter in determining the heat transfer performance of jet impingement cooling systems. Higher Nusselt numbers are usually shown at smaller H/B values due to stronger stagnation effects and enhanced turbulence near the impingement region (Yang et al., 2011). In the present study, it is illustrated that at lower H/B values, which is H/B = 0.5, the Nusselt number is highest among others. As the H/B ratio increases, the impinging jet travels a longer distance before reaching the target surface, causing it to lose momentum and turbulence due to mixing with the surrounding fluid. The Nusselt number gradually decreases and begins to stabilise beyond H/B = 2. These findings indicate that incremental gains in heat transfer become small with increasing H/B as shown in Table 4. The results are consistent with the distribution of turbulence kinetic energy in the contour fields as shown in Fig. 4.

Table 4. Relative error for CFD model validation

Jet-to-surface distance (H/B)	**Maximum turbulent kinetic energy ($m^2 \cdot s^{-2}$)**
0.50	82.28
2.00	25.84
5.00	62.83
8.00	59.07

Source: Author's own data

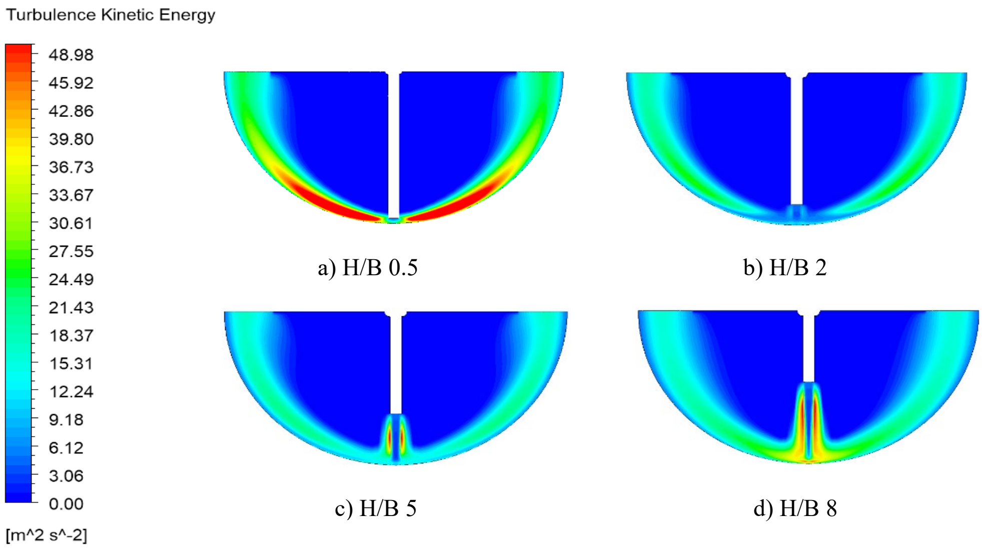

Fig. 4. Turbulent kinetic energy contour for H/B effect

Source: Author's own data

The highest turbulent kinetic energy of 82.28 $m^2 \cdot s^{-2}$ at H/B 0.5, shows an intense turbulence concentrated near the stagnation region and wall jet. This condition produces strong mixing and enhanced convective heat transfer. Increasing the spacing to H/B = 2.00 leads to a sharp reduction in turbulent kinetic energy to 25.84 $m^2 \cdot s^{-2}$, corresponding to a decrease of approximately 69% due to jet momentum dissipation and weakened turbulence production at the stagnation zone. At H/B = 5.00, turbulent kinetic energy increases again to 62.83 $m^2 \cdot s^{-2}$, indicating partial recovery of turbulence intensity driven by shear layer development.

For H/B = 8.00, the turbulent kinetic energy slightly decreases to 59.07 $m^2 \cdot s^{-2}$, with the turbulence field dominated by wall shear rather than stagnation effects due to substantial jet core dissipation before impact. Overall, smaller H/B maximises turbulence intensity, while increasing H/B results in progressive momentum decay and reduced stagnation region turbulence. Based on these observations, H/B = 0.5 is identified as the optimal spacing, as it provides the most effective combination of turbulence generation and heat transfer enhancement. Consequently, this configuration is selected for subsequent analyses involving variations in Reynolds number.

Effect of Reynold number

The Reynolds number analysis was conducted at a constant jet-to-surface distance ratio of H/B = 0.5, as this configuration produced the maximum Nusselt number. To separate the effect of Reynolds number on flow behaviour and thermal performance, the H/B ratio was kept the same while the Reynolds number was changed in a systematic way. Table 5 shows the Nusselt number and maximum turbulent kinetic energy values that were found in simulations with Reynolds numbers of 5000, 25000, and 45000. This enables a direct assessment of heat transfer enhancement associated with increased flow momentum and turbulence intensity.

Table 5. Effect of Reynold number on Nusselt number and maximum turbulent kinetic energy

Reynold number	Velocity inlet (m/s)	Nusselt number	Maximum turbulent kinetic energy ($m^{2}\cdot s^{-2}$)
5000	7.80	34.33	4.68
25000	38.99	89.31	98.89
45000	70.18	123.16	302.45

Source: Author's own data

These results clearly indicate that the Reynolds number is directly proportional to both the Nusselt number and the maximum turbulent kinetic energy. As the Reynolds number increases, the impinging jet carries higher momentum and exhibits greater turbulence intensity, which enhances the entrainment of surrounding fluid and leads to the formation of stronger shear layers (Conahan, 2021). As a result, heat transfer performance improves due to increased convective transport and elevated turbulence levels. It is consistent with the observations of Xu et al. (2010), who reported that higher Reynolds numbers promote stronger flow instabilities, more effective turbulent mixing, and steeper thermal gradients in the stagnation region. The turbulent kinetic energy contours presented in Fig. 5 supports these trends.

Fig. 5(a) at Re = 5000 shows weak and limited turbulence in space, which limits the overall cooling performance. Fig. 5(b), on the other hand, shows a significant rise in turbulent kinetic energy at Re = 25000. This energy is more concentrated near the impingement area, which leads to better fluid mixing and stronger interaction with the surface. The red contours that form near the wall jet region in Fig. 5(c) at Re = 45000 show that turbulent kinetic energy is at its highest point. These findings indicate that elevating the Reynolds number exacerbates turbulence, resulting in enhanced mixing and an enlargement of the active cooling zone. The highest Reynolds number also shows the strongest wall jet renewal, which is in line with Ajeel et al. (2024)'s findings of increased convective transport and higher Nusselt numbers.

Effect of nozzle diameter

The study continues with an analysis of nozzle diameter as a key parameter influencing jet impingement cooling performance. Simulations were performed using three different nozzle diameters of 5 mm, 10 mm, and 25 mm across all jet to surface distance ratios (H/B). Table 6 presents the effects of nozzle diameter on the Nusselt number and turbulent kinetic energy.

At fixed diameter, Nusselt number decreases with larger H/B for D = 15 mm (170.77 to 71.69 $m^2 \cdot s^{-2}$) and for D = 10 mm (145.71 to 77.05 $m^2 \cdot s^{-2}$). Meanwhile, an increasing diameter from 5 to 15 mm increases the Nusselt number from 86.58 to 170.77 $m^2 \cdot s^{-2}$ (97% increase). This finding is consistent Huang et al. (2021) study, reported that increasing nozzle diameter improves heat transfer uniformity. The thermal gradients reduced over the target surface while maintaining high local Nusselt numbers near the stagnation region (Huang et al., 2021).

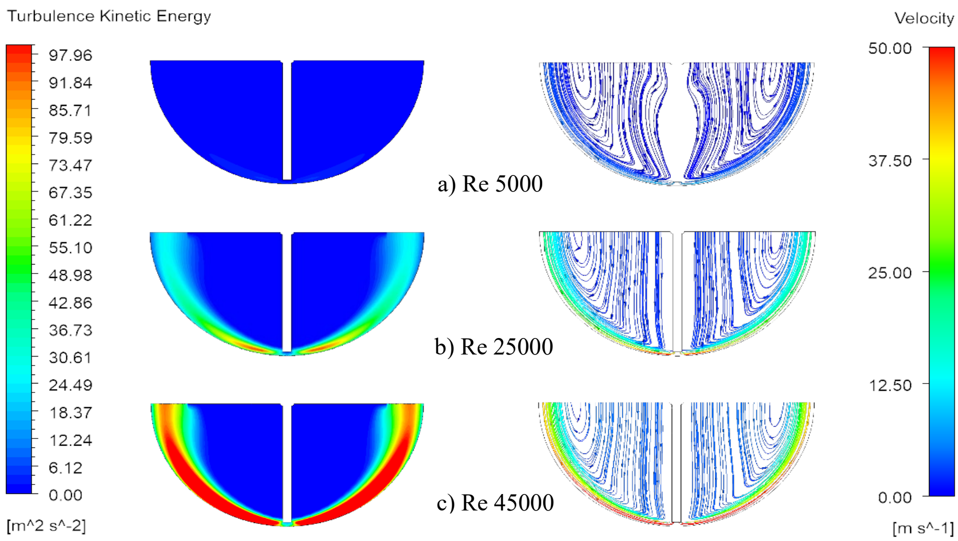

Fig. 5. Turbulent kinetic energy for Reynold number effect

Source: Author's own data

Table 6. Effect of nozzle diameter on Nusselt number and turbulent kinetic energy

Jet-to-surface distance (H/B)	Jet length, H (mm)	Effect of diameter (mm) on Nusselt number			Effect of diameter (mm) on turbulent kinetic energy ($m^2 \cdot s^{-2}$)		
		5	10	15	5	10	15
0.50	72.5	86.58	145.71	170.77	82.28	464.74	1093.91
2.00	65	76.18	91.5	107.19	25.84	58.04	92.88
5.00	50	72.32	76.47	76.97	62.83	37.36	46.35
8.00	40	71.56	77.05	71.69	59.07	57.11	37.85

Source: Author

4. CONCLUSION

This research successfully achieved the objectives to analyse the nozzle configuration effect on jet impingement cooling performance. The study revealed that nozzle diameter, Reynolds number, and jet-to-surface distance have a significant impact on the cooling process of the concave surface. An increase in Reynolds number led to a higher Nusselt number, indicating improved cooling efficiency due to increased turbulence within the impinging jet. Similarly, larger nozzle diameters expanded the jet impingement area and also contributed to a higher Nusselt number. In comparison, a larger jet-to-surface distance (H/B) decreases the Nusselt number due to decay of jet momentum and turbulence intensity before impact. Therefore, the results verify that controlling these parameters is essential for achieving efficient and uniform cooling with impinging jets. These findings highlight the contribution to the design of cost-effective and high-performance cooling systems, particularly in industrial applications where localised heat removal is employed.

ACKNOWLEDGEMENTS

The authors would like to acknowledge the support of Universiti Teknologi MARA, Shah Alam, Selangor, Malaysia, and the Faculty of Engineering and Built Environment, Universiti Kebangsaan Malaysia, Selangor, for providing the facilities for this research.

FUNDINGS

This research received no external funding.

CONFLICT OF INTEREST STATEMENT

The authors agree that this research was conducted in the absence of any self-benefits, commercial or financial conflicts and declare the absence of conflicting interests with the funders.

AUTHORS' CONTRIBUTIONS

Nurul Hyidayah Shahrin: Conceptualisation, methodology, formal analysis, investigation and writing-original draft; **Nadia Kamarrudin:** Conceptualisation, methodology, formal analysis, supervision, writing-review and editing; **Masli Irwan Rosli:** Conceptualisation and validation; **Mohd Fadhil Majnis:** writing-review and editing.

DECLARATION OF GENERATIVE AI IN THE WRITING PROCESS

During the preparation of this work, the author(s) used ChatGPT in order to generate ideas and improve clarity. After using this tool/service, the author(s) reviewed and edited the content as needed and take(s) full responsibility for the content of the publication.

DATA AVAILABILITY/SUPPLEMENTARY MATERIALS

The datasets used and/or analysed during the current study are available from the corresponding author on reasonable request.

ETHICAL COMPLIANCE STATEMENT

The authors confirm that the research was conducted with integrity, and all data were reported accurately without fabrication, falsification, or inappropriate manipulation

ETHICS APPROVAL STATEMENT

The authors declare that this study did not involve human or animal subjects and complies with institutional ethical guidelines.

REFERENCES

Ajeel, R. K., Fayyadh, S. N., Sopian, K., Sultan, S. M., Salim, W. S. I. W., & Tso, C. P. (2024). Multiple impingement jets with binary hybrid nanofluids: Performance assessment of flow and heat transfer characteristics. *Journal of Thermal Analysis and Calorimetry*, *149*(17), 9903-9920. https://doi.org/10.1007/s10973-024-13374-3

Attalla, M., & Salem, M. (2013). Effect of nozzle geometry on heat transfer characteristics from a single circular air jet. *Applied Thermal Engineering*, *51*(1–2), 723–733. https://doi.org/10.1016/j.applthermaleng.2012.09.032

Baonga, J. B., Louahlia-Gualous, H., & Imbert, M. (2006). Experimental study of the hydrodynamic and heat transfer of free liquid jet impinging a flat circular heated disk. *Applied Thermal Engineering*, *26*(11–12), 1125–1138. https://doi.org/10.1016/j.applthermaleng.2005.11.001

Basha, S.E., Prasad, K. L., Kartheek, G. & Viswanath, K. V. (2018). Experimental analysis of jet impingement on aluminium heat sink. *International Journal of Mechanical Engineering and Technology*, 9(6), 1129–1140. http://iaeme.com/Home/issue/IJMET?Volume=9&Issue=6

Choo, K., & Kim, S. J. (2016). The influence of nozzle diameter on the circular hydraulic jump of liquid jet impingement. *Experimental Thermal and Fluid Science*, *72*, 12–17. https://doi.org/10.1016/j.expthermflusci.2015.10.033

Conahan, J. M. (2021). High Reynolds number millimeter-scale jet impingement phenomena. [Master Thesis, Northeastern University]. Northeastern University Repository. https://repository.library.northeastern.edu/files/neu:bz60w8443/fulltext.pdf

Ekkad, S. V. & Singh, P. (2021). A modern review on jet impingement heat transfer methods. *ASME Journal of Heat and Mass Transfer*, *143*(6), 064001. https://doi.org/10.1115/1.4049496

Erasmus, D.J., Lubkoll, M. & Backström, T.W.V. (2021). Jet impingement heat transfer within a hemisphere. *Heat Mass Transfer*, *57*, 931–948. https://doi.org/10.1007/s00231-020-02977-9

Garimella, S. V. & Nenaydykh, B. (1996). Nozzle-geometry effects in liquid jet impingement heat transfer. *International Journal of Heat and Mass Transfer*, *39*(14), 2915-2923. https://doi.org/10.1016/0017-9310(95)00382-7

Huang, T., Tan, P., Zhang, Y., Huang, Z., & Zhou, H. (2021). Heat transfer uniformity analysis of floatation nozzle using a revised uniformity indicator. *International Journal of Heat and Mass Transfer*, *168*, 120885. https://doi.org/10.1016/j.ijheatmasstransfer.2020.120885

Janajreh, I., Ghenai, C., & Sarfraz, O. (2014). Numerical simulation of internal channel cooling via jet impingement in fluent and its sensitivity study. *10th International Conference on Heat Transfer, Fluid Mechanics and Thermodynamics*. http://hdl.handle.net/2263/44687

Kund, M. (2019). Numerical study on effect of nozzle size for jet impingement cooling with water–Al_2O_3 nanofluid. *International Journal of Engineering and Advanced Technology*, *8*(4), 736-739. https://www.ijeat.org/wp-content/uploads/papers/v8i4/D6257048419.pdf

Patil, V. S., & Vedula, R. P. (2018). Local heat transfer for jet impingement onto a concave surface including injection nozzle length to diameter and curvature ratio effects. *Experimental Thermal and Fluid Science, 92*, 375–389. https://doi.org/10.1016/j.expthermflusci.2017.08.002

Prevost, T., Battaglioli, S., Jenkins, R., & Robinson, A. J. (2022). Enhancing jet array heat transfer: Review of geometric features of nozzle and target plates. *International Journal of Thermofluids*, *16*, 100203. https://doi.org/10.1016/j.ijft.2022.100203

Rakhsha, S., Zargarabadi, M. R., & Saedodin, S. (2023). The effect of nozzle geometry on the flow and heat transfer of pulsed impinging jet on the concave surface. *International Journal of Thermal Sciences*, *184*, 107925. https://doi.org/10.1016/j.ijthermalsci.2022.107925

Versteeg, H. K. & Malalasekera, W. (2007). *An introduction to computational fluid dynamics the finite volume method* (2nd ed.). Pearson Education Limited.

Xu, P., Yu, B., Qiu, S., Poh, H. J., & Mujumdar, A. S. (2010). Turbulent impinging jet heat transfer enhancement due to intermittent pulsation. *International Journal of Thermal Sciences*, *49*(7), 1247–1252. https://doi.org/10.1016/j.ijthermalsci.2010.01.020

Yang, G., Choi, M., & Lee, J. S. (1999). An experimental study of slot jet impingement cooling on concave surface: Effects of nozzle configuration and curvature. *International Journal of Heat and Mass Transfer*, *42*(12), 2199-2209. https://doi.org/10.1016/S0017-9310(98)00337-8

Yang, Y. T., Wei, T. C., & Wang, Y. H. (2011). Numerical study of turbulent slot jet impingement cooling on a semi-circular concave surface. *International Journal of Heat and Mass Transfer*, *54*(1–3), 482–489. https://doi.org/10.1016/j.ijheatmasstransfer.2010.09.021